Experimental and Numerical Analysis of a PCM-Integrated Roof for Higher Thermal Performance of Buildings

François Simon, Letzai Ruiz-Valero, Aymeric Girard, Hector Galleguillos

Experimental and Numerical Analysis of a PCM-Integrated Roof for Higher Thermal Performance of Buildings

SIMON François[1*], RUIZ-VALERO Letzai[2], GIRARD Aymeric[3,4], GALLEGUILLOS Hector[5]

1. Centro de Desarrollo Urbano Sustentable (CEDEUS), Pontificia Universidad Católica de Chile, 7500000 Santiago, Chile
2. Facultad de Ciencias e Ingeniería, Pontificia Universidad Católica Madre y Maestra (PUCMM), 10103 Santo Domingo, Dominican Republic
3. LMGC, IMT Mines Ales, Univ Montpellier, CNRS, 30100 Alès, France
4. Facultad de Ingeniería y Ciencias, Universidad Adolfo Ibañez, 2520000 Viña del Mar, Chile
5. Centro de Desarrollo Energético Antofagasta (CDEA), Universidad de Antofagasta, 1240000 Antofagasta, Chile

Abstract: Phase change materials (PCMs) designate materials able to store latent heat. PCMs change state from solid to liquid over a defined temperature range. This process is reversible and can be used for thermo-technical purposes. The present paper aims to study the thermal performance of an inorganic eutectic PCM integrated into the rooftop slab of a test room and analyze its potential for building thermal management. The experiment is conducted in two test rooms in Antofagasta (Chile) during summer, fall, and winter. The PCM is integrated into the rooftop of the first test room, while the roof panel of the second room is a sealed air cavity. The work introduces a numerical model, which is built using the finite difference method and used to simulate the rooms' thermal behavior. Several thermal simulations of the PCM room are performed for other Chilean locations to evaluate and compare the capability of the PCM panel to store latent heat thermal energy in different climates. Results show that the indoor temperature of the PCM room in Antofagasta varies only 21.1°C±10.6°C, while the one of the air-panel room varies 28.3°C±18.5°C. Under the experiment's conditions, the PCM room's indoor temperature observes smoother diurnal fluctuations, with lower maximum and higher minimum indoor temperatures than that of the air-panel room. Thermal simulations in other cities show that the PCM panel has a better thermal performance during winter, as it helps to maintain or increase the room temperature by some degrees to reach comfort temperatures. This demonstrates that the implementation of such PCM in the building envelope can effectively reduce space heating and cooling needs, and improve indoor thermal comfort in different climates of Chile.

Keywords: phase change material; thermal energy storage; building; space heating and cooling; energy efficiency; designbuilder

Nomenclature

Latin symbols

Cp	Specific heat capacity/J·(kg·K)$^{-1}$
h	Coefficient of convection/W·(m^2·K)$^{-1}$
k	Thermal conductivity/W·(m·K)$^{-1}$
L	Length of the panel/m
q	Irradiation/W·m^{-2}
T	Temperature/°C
t	Time
x	System abscise/m

Greek symbols

α	Absorptivity
ε	Emissivity
ρ	Density/kg·m^{-3}
σ	Stefan-Boltzmann constant/W·m^{-2}·K^{-4}

Subscripts

air	Air in the panel
i	Volume cell number
in	Inside
m	Correspondent material
o	Outside
PCM	PCM in the panel
s	Sun
si	Inner surface
sky	Sky
so	Outer surface
∞	Outside ambient air

Dimensionless number

f	Implicit coefficient
Gr	Grashoff number
Nu	Nusselt number
Pr	Prandtl number
Re	Reynolds number

1. Introduction

The energy consumption of the building sector (commercial, public, and residential) accounted for 23% of the total primary energy consumption in Chile with 6.5 million tons of oil equivalent (Mtoe) in 2020, according to the Ministry of Energy [1]. Since more than half of this (53%) is attributed to space heating and cooling [2], the thermal performance of building envelopes played an important role in the energy conservation of buildings [3].

A sustainable built environment requires buildings to be constructed with energy-efficient envelope materials to achieve low heating and cooling loads [4]. One energy-saving concept is to use latent heat storage in phase change materials (PCMs) within the building envelope for space thermal control [5, 6]. It has been demonstrated that PCM-enhanced building envelopes offer higher heat capacity per unit volume than conventional building materials [7] and provide the benefit of increased thermal inertia [8, 9].

PCMs store incoming thermal energy in the form of latent heat as the ambient temperature increases above their melting point and reject it when the ambient temperature drops below their freezing point [10]. This form of thermal energy storage is due to the energy associated with the molecules bonded to each other. Thermal energy is released when the bonds break or new bonds are formed. It is dependent on the type of reaction, the materials involved, and the extent of the reaction [11]. The use of active thermal PCM within the building envelope can smooth the temperature fluctuations of interior space, lower the space heating/cooling energy consumption of buildings, and improve the thermal comfort of the indoor environment [12–17]. This is due to PCM's high energy storage density and approximate stationary temperature when the phase change takes place [18–20].

PCMs received considerable attention recently, particularly in exploring the effectiveness of PCMs in improving indoor thermal comfort in buildings [5, 21]. However, despite the extensive research about PCM applications in buildings [22], a lot of work remains for PCMs to fulfill certain fundamental criteria practically and reliably:

(1) PCM selection: Efforts are still needed to establish material suitability depending on PCM thermo-physical characteristics to match load requirements for different types and shapes of buildings, in different climate areas and during different seasons. The most appropriate melting temperature, the latent heat of fusion, and the heat conductivity of PCMs must be the first consideration [23].

(2) PCM application within the building envelope: Direct immersion and impregnation of building envelope elements are the simplest and most economical methods [24], but micro-encapsulation of PCMs, particularly shape-stabilized PCMs, is a promising technic due to its effectiveness in reducing the danger of leakage as well as its relatively low cost [25]. Yet, the ratio of PCM-to-conventional materials in the building envelope, the position, and the thickness of PCM panels depend on the building's architectural characteristics, and the location climate. It is fundamental to optimize these parameters to achieve successful PCM applications in buildings.

(3) Safety and long-term behavior: Aspects of safety

such as mechanical destruction limit of structure [26], and high flammability [27] are important issues, which can limit the commercial viability of PCMs. There is a need to evaluate experimentally the durability of PCM building elements, their long-term thermal behavior, and their fire-resistance rating. Also, PCMs should not pose a risk to living health or the environment.

(4) Heat transfer enhancement: Efforts are still in demand to improve PCM thermal conductivity, reduce inadequate heat transfer during the phase change process, and eliminate supercooling [28, 29].

The present paper aims to study the thermal performance of a non-toxic inorganic eutectic PCM (48% $CaCl_2$+4.3% NaCl+0.4% KCl+47.3% H_2O, mass ratio) integrated into the rooftop slab of a test room and analyze its potential for building thermal management in different Chilean climates. The investigation is performed through an experiment in two test rooms in Antofagasta (Chile) during summer, fall, and winter. The PCM is integrated into the first test room's rooftop slab, while the second room's roof panel is a sealed air cavity. Except for their rooftop composition, both test rooms have identical design characteristics to evaluate the effect of the PCM on the room's thermal behavior.

The paper contributes to filling the gap in experimental and numerical investigation related to the use of the studied PCM for latent heat thermal energy storage and energy conservation in Chilean buildings. For that purpose, the work introduces a numerical model built using the finite difference method (FDM) to simulate the thermal behavior of both test rooms. The proposed model is verified using DesignBuilder software and validated with experimental findings. Then, several thermal simulations of the PCM room are performed for other Chilean locations to evaluate and compare the capability of the PCM panel to store latent heat thermal energy in different climates. The paper provides scientifically-based evidence that the incorporation of the mentioned PCM into the building envelope can effectively reduce the energy demand for space heating and cooling in different climates of Chile.

2. Materials and Methods

2.1 General climate conditions

The experimentation was carried out in Antofagasta, which is located in northern Chile between 21°28′ and approximately 25°55′ south latitude. The regional surface has a length of approximately 500 kilometers and covers an area of 126 049 square kilometers. This region has an arid climate, hydrographic scarcity, little vegetation, and a relief similar to the rest of the country [30]. The average temperature ranges between 9.2°C and 26°C, with an average annual precipitation of 3 mm and an annual precipitation of 10 mm [31]. It has an average wind speed of 9.6 km/h [32]. Regarding solar potential, Antofagasta has a daily global horizontal irradiation of 5.96 kWh/m^2, normal direct radiation of 6.74 kWh/m^2, and diffuse horizontal radiation of 1.73 kWh·m^{-2} [33]. Fig. 1 shows air temperature and normal direct solar radiation for a typical year in Antofagasta.

In addition, to compare the behavior of the PCM in other climates, different regions of continental Chile have been considered, each representing a different climate. Chile has a wide range of climate zones [35], due to its large extension from north to south (i.e. from 23.4S latitude in Antofagasta to 53.2S latitude in Punta Arenas). Thus, one city was selected for each of the main climate zones of Chile. Table 1 presents the climate information of the selected cities.

2.2 Experimental set-up

Two experimental test rooms (1.14 m×1.14 m×1.65 m) have been built to investigate the potential of a rooftop PCM panel for latent heat thermal energy storage and energy conservation. Both rooms have identical

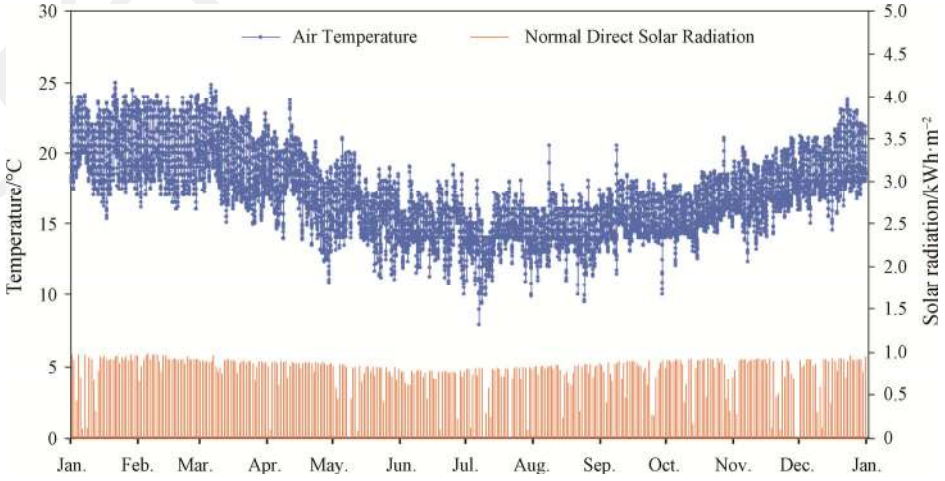

Fig. 1 Climate conditions for a typical year in Antofagasta [34]

Table 1 Climate zones [31, 33, 35]

City	Zone	Climate	Average temperature ranges/°C	Daily global horizontal radiation/kWh·m^{-2}	Daily normal direct radiation/ kWh·m^{-2}	Daily diffuse horizontal radiation/kWh·m^{-2}
Antofagasta	North Coast	Desert with maritime dominance	9.2–26	5.96	6.74	1.73
Calama	North Desert	Desert	0.4–21.2	7.41	10.85	0.70
Copiapó	North Transversal Valleys	Semi Desert	6.2–29.4	6.44	8.90	0.78
Valparaiso	Central Coast	Maritime	7.2–25.8	4.91	5.83	1.45
Santiago	Central Inland	Mediterranean	4.2–30.6	5.32	6.95	1.20
Concepción	South Coast	Maritime and rainy	2.9–26.4	4.85	6.44	1.19
Temuco	South Inland	Rainy and cold with frequent frosts	4.7–23	4.26	5.31	1.33
Punta Arenas	Extreme South	Rainy and cold	0.1–10.3	3.16	4.73	1.22

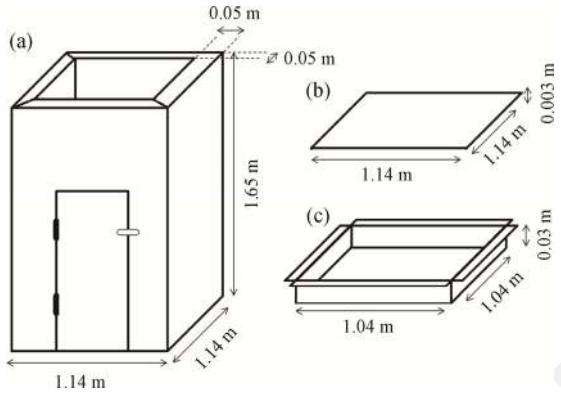

Fig. 2 Experimental room dimensions: (a) room, (b) rooftop, (c) PCM/air panel

construction characteristics. The walls consist of 50 mm sandwich panels (R=1.6 m^2·K·W^{-1}) composed of three layers, an external and internal stainless steel plate, and a high-density expanded polystyrene foam core. The floor is made of 15 mm plywood. The rooftop slab consists of an airtight stainless steel cavity (1.04 m×1.04 m×0.03 m) (Fig. 2), containing air in one room and the inorganic eutectic PCM under study (48% $CaCl_2$+4.3% NaCl+0.4% KCl +47.3% H_2O) in the other room. The stainless steel rooftop cavity in both rooms is airtight. This is to avoid heat transfer through ventilation on one side and maintain the PCM integrity on the other side, as excess moisture can alter the PCM composition and performance. The experiment is set up in the location of Antofagasta, Chile. The properties of the PCM used in the experiment are given in Table 2.

The PCM mixture is prepared by mixing the inorganic salts in the appropriate proportion of $CaCl_2$, NaCl, and KCl with the correct quantity of distilled water. The mixture is then agitated properly until the salts are completely diluted in the distilled water. The KCl and NaCl salts help to initiate nucleation and to prevent incongruent melting and sub-cooling. The total mass of the PCM mixture used is 53.2 kg, which, is poured in its liquid state into the panel, and the whole assembly is sealed properly (Fig. 3).

Table 2 Technical characteristics of the studied PCM [36, 37]

PCM composition	48% $CaCl_2$+4.3% NaCl +0.4% KCl+47.3% H_2O
Appearance (color)	Grey
Phase change temperature/°C	26–28
Density/kg·m^{-3}	1640
Latent heat of fusion/kJ·kg^{-1}	188
Thermal conductivity/W·(m·K)$^{-1}$	
Solid	1.09 (0–27°C)
Liquid	0.54 (28°C–60°C)
	1440 (0–26.5°C)
Specific heat/J·(kg·K)$^{-1}$	125,000 (26.5°C–28°C)
	1440 (28°C–60°C)

Fig. 3 Installation of test rooms with and without PCM

The resistance temperature detectors (type PT100) are placed in different depths in the PCM panel with perfect sealing (Fig. 4). Temperatures and solar global irradiation are recorded using a digital data logger at 30-minute intervals for both test rooms during the months of March (summer), May (fall), and July (winter). These data

include the exterior air temperature, roof outer, and inner surface temperatures, the air gap and PCM temperatures, and the room indoor temperatures.

Fig. 4 Temperature sensors set-up

2.3 Numerical model

The proposed model is built using the finite difference method (FDM) to simulate the experiment. It consists in reproducing numerically the behavior of the selected PCM and air panels in the structure configuration shown in Fig. 5. For simulation purposes, the structure is divided into nine finite volume cells, each element divided into three volume cells. Both the PCM and air panels placed on the top horizontal surface of the corresponding test room are studied for thermal behavior comparison. As defined by the FDM, median temperature values on each cell constituting the system are calculated. These median values represent the temperature in the middle of each cell.

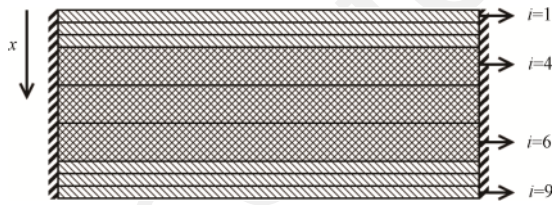

Fig. 5 Finite volume grid for the analysis

For convection, the heat transfer coefficient (h) value on the outer surface is calculated based on the prevailing velocity of the wind using the Nusselt correlation. Regarding the parameters involved, it is important to note that the Nusselt number is equal to the intensity of the convection times the characteristic length of the studied system, divided by the thermal conductivity of the engaged fluid, which can be calculated using the following Equation (1).

$$Nu = \frac{hL}{\lambda} \tag{1}$$

The Nusselt number can be calculated using Eq. (2) for the upper surface, and Eq. (3) for the lower surface.

$$Nu = 0.664 Re^{0.5} Pr^{0.33} \tag{2}$$

$$Nu = 0.54 \left(GrPr\right)^{0.25} \tag{3}$$

The respective exterior and interior convection coefficients are taken equal to 18 and 5 $W\cdot(m^2\cdot K)^{-1}$, as shown in Table 3, where all physical data and assumptions are detailed. We note that the implicit factor f is a dimensionless number, which can be calculated using Eq. (4).

$$f = \frac{k\mathrm{d}t}{\rho Cp\mathrm{d}x^2} \tag{4}$$

Table 3 Physical data used in the simulation

x steel/m	0.003	x gap/m	0.03
dx steel/m	0.001	dx gap/m	0.01
ρ steel/kg·m^{-3}	7860	ρ air/kg·m^{-3}	1.23
Cp steel/J·(kg·K)$^{-1}$	500	Cp air/J·(kg·K)$^{-1}$	1000
k steel/W·(m·K)$^{-1}$	52	k air/W·(m·K)$^{-1}$	0.024
h_{so}/W·(m^2·K)$^{-1}$	18	h_{si}/W·(m^2·K)$^{-1}$	5
dt/s	1800	σ	5.67E–8
ε	0.9	α	0.6
f solid	0.923	f liquid	0.457

The following introduces the statement of the studied system and the mathematical formulation including the development of the governing equations for all modes of heat transfer and the boundary conditions. It is important to note that the thermal equations must be adapted to numerical equations by approximating the derivatives with the Taylor formula.

2.3.1 Heat transfer process

The heat transfer processes are studied over 48-hour periods. This means that all thermal exchanges are involved (i.e. radiation, convection, and conduction). During sunshine hours, solar radiation is heating the constructions from the top. Then, a thermal potential difference is engaged, involving three main processes (Fig. 6). First, due to variable thermo-properties, the temperature difference between the top surface and the outside ambient air induces a phenomenon of heat transfer by natural convection at the outside surface of the room's roofs. Then, the temperature difference between the inner and outer surfaces of the system generates conduction through the three materials of the roof panel. Finally, heat transfer by natural convection occurs between the inside roof surface and the internal air.

During sunshine hours (charging process), the PCM within the stainless-steel panel changes its phase from solid to liquid. During the night hours (discharging process), because of the absence of direct incident solar radiation and cooler ambient temperatures, the PCM solidifies (i.e. its

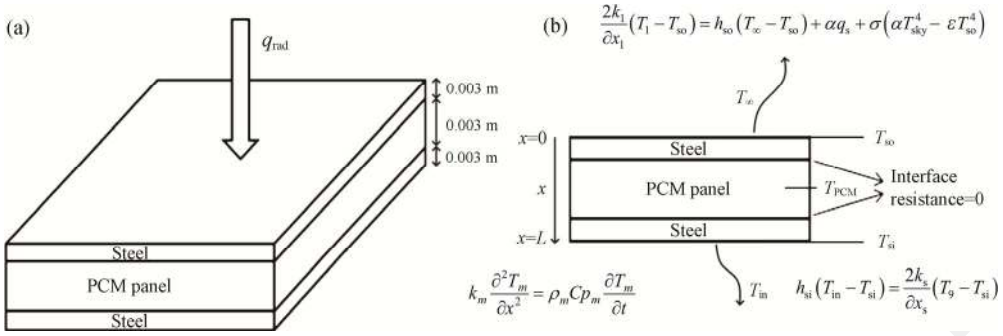

Fig. 6 Diagram of the system physics

phase changes from liquid to solid) and rejects its heat to the surroundings, specifically to the outside ambient and the air inside the test room. The PCM phase change cycle is repeated every day.

2.3.2 Governing equations and boundary conditions

The engaged equation is the heat equation simplified to a unidirectional and temporal equation applied to a solid. This means that no velocity is involved and only one dimension is used in the direction of the heat transfer, as shown in Fig. 5. For that purpose, we assume that the thermal flow is one-dimensional, that there is no interfacial resistance between the different panels of steel and PCM, and that the thermal conductivity of the steel sheets is constant. We also assume that the PCM is homogeneous and isotropic and that the convection effect in the molten PCM is neglected.

According to the mentioned assumptions, the governing equations are developed as follows.

$$\rho Cp \frac{\partial T}{\partial t} = k \frac{\partial^2 T}{\partial x^2} \tag{5}$$

Exterior boundary condition (x=0):

$$\frac{2k_1}{\partial x_1}(T_1 - T_{so}) = h_0 (T_\infty - T_{so}) + \alpha q_s + \sigma\left(\alpha T_{sky}^4 - \varepsilon T_{so}^4\right) \tag{6}$$

Interior boundary condition (x=L):

$$h_{si}(T_{in} - T_{si}) = \frac{2k_s}{dx_s}(T_9 - T_{si}) \tag{7}$$

Now we have to define the equations governing each of the nine nodes of the system. First, we remind that Taylor proposes to linearize the second-order derivate as follows.

$$\frac{\partial^2 T}{\partial x^2} \approx \frac{T_{i-1} - 2T_i + T_{i+1}}{\partial x^2} \tag{8}$$

Exterior node. The equation of volume cell 1 can be written as in Eq. (9).

$$\begin{aligned} \frac{\rho_1 Cp_1 dx_1}{dt}\left(T_1 - T_1^0\right) = (1-2f)\frac{k_1}{dx_1}(T_2 - T_1) \\ - h_{so}(T_{so} - T_\infty) + \alpha q_s \\ + \sigma\left(\alpha T_{sky}^4 - \varepsilon T_{so}^4\right) \end{aligned} \tag{9}$$

where T_1^0 stands for the previous time step temperature at the first volume cell. ρ_1, Cp_1, and k_1 are the physical characteristics of the rooftop material (i.e. steel). T_{sky} equals $0.0552 T_\infty^{1.5}$.

Inner node. The equation of the volume cells located in between the top and bottom volume cells of a particular material (i.e. for cell i=2, 5, 8) can be expressed as follows.

$$\begin{aligned} \frac{\rho_m Cp_m dx_m}{dt}\left(T_i - T_i^0\right) = (1-2f)\frac{k_m}{dx_m}(T_{i+1} - T_i) \\ - \frac{k_m}{dx_m}(T_i - T_{i-1}) \end{aligned} \tag{10}$$

where T_i^0 stands for the previous time step temperature at i^{th} volume cell. ρ_m, Cp_m, and k_m are the physical characteristics of the corresponding material m (i.e. steel, PCM, or air).

Interface node. The equation of the volume cell i=3, 6 can be written as in Eq. (11) below.

$$\begin{aligned} \frac{\rho_1 Cp_1 dx_1}{dt}\left(T_i - T_i^0\right) = (1-2f)\frac{1}{\frac{dx_1}{2k_1} + \frac{dx_2}{2k_2}}(T_{i+1} - T_i) \\ - \frac{k_i}{dx_i}(T_i - T_{i-1}) \end{aligned} \tag{11}$$

where ρ_1, Cp_1, k_1, and k_2 are the material physical characteristics. For cell i=3, subscripts 1 and 2 represent the rooftop steel and the PCM/air panel respectively; for cell i=6, subscripts 1 and 2 represent the PCM/air panel and the steel (bottom layer) respectively.

The equation of the volume cell i=4, 7 can be expressed as follows.

$$\begin{aligned} \frac{\rho_2 Cp_2 dx_2}{dt}\left(T_i - T_i^0\right) = (1-2f)\frac{k_i}{dx_i}(T_{i+1} - T_i) \\ - \frac{k_i}{\frac{dx_1}{2k_1} + \frac{dx_2}{2k_2}}(T_i - T_{i-1}) \end{aligned} \tag{12}$$

where ρ_1, Cp_1, k_1, and k_2 are the material physical characteristics. For cell i=4, subscripts 1 and 2 represent the rooftop steel and the PCM/air panel respectively; for cell i=7, subscripts 1 and 2 represent the PCM/air panel

and the steel (bottom layer) respectively.

Interior node. The equation of the volume cell 9 can be written as in Eq. (13).

$$\frac{\rho_3 Cp_3 \mathrm{d}x_3}{\mathrm{d}t}\left(T_9 - T_9^0\right) = \left(1-2f\right)h_{\mathrm{si}}\left(T_{\mathrm{in}} - T_{\mathrm{si}}\right) - \frac{k_3}{\mathrm{d}x_3}\left(T_9 - T_8\right) \tag{13}$$

where ρ_3, Cp_3, and k_3 are the physical characteristics of the bottom layer material (steel).

2.4 Simulation model verification

We use DesignBuilder v.5.0.2.3 [34] for the verification of the proposed model. The DesignBuilder software package is recognized as the most comprehensive user interface for EnergyPlus [38] and it is widely used in building environmental and energy simulations. This software package enables the performance of dynamic simulations via version 8.7.0 of the Energy Plus numerical engine [39], which uses a one-dimensional conduction finite difference (CondFD) solution algorithm to perform dynamic simulations of materials with variable thermal properties such as PCMs. This solution algorithm employs the same FDM as the proposed model detailed in the previous section. In DesignBuilder, we chose to apply the fully implicit finite difference scheme, combined with an enthalpy-temperature function [40–42]. A flow chart of the simulation process is shown in Fig. 7.

A test room was created in DesignBuilder (Fig. 8), and PCMs were modeled as a separate element and added to the building system. The model considers some thermal-physical properties for each of the materials involved, e.g., conductivity, thickness, density, specific heat, and some specific properties like the PCM temperature-enthalpy function.

Table 4 shows the material characteristics of the test rooms and describes the layers that comprise the roof, walls, and floor. In addition, the thermal transmittance of each element is shown. For the modeling, we use the ASHRAE 55-2013 standard and simulate the experiment as a passive system to evaluate the behavior of the PCM. The technical characteristics of the PCM are described in Table 2. However, for the simulation, the temperature-enthalpy function of the BioPCM M27/Q21 is taken as a reference because it has similar properties to the PCM used in the experiment (Table 5).

The simulation was carried out for both test rooms (i.e. the one including the PCM, and the one including the air panel) for Antofagasta to verify its validity against the experimental results. While for the other cities introduced in Table 1, the simulation was done for the PCM test room only, so that the thermal performance and behavior of this material can be evaluated in different climatic zones.

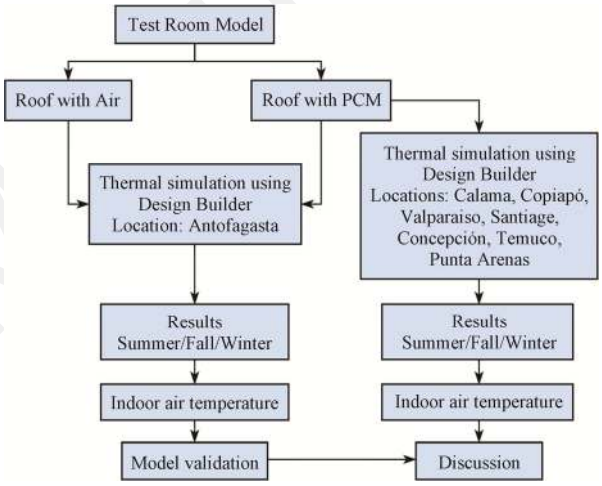

Fig. 7 Flow chart of the simulation

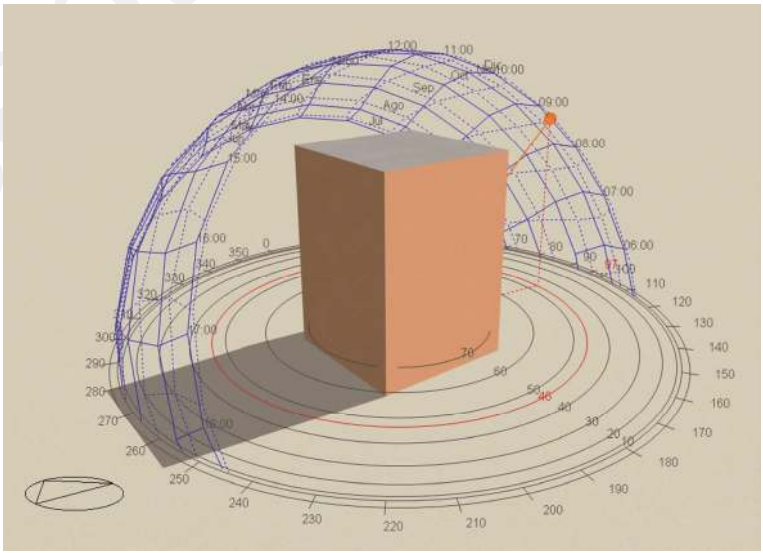

Fig. 8 Test room in DesignBuilder

Table 4 Test room material characteristics [43]

	Thickness/ m	Material	k Conductivity/ $W\cdot(m\cdot K)^{-1}$	ρ Density/ $kg\cdot m^{-3}$	Cp Specific heat/$J\cdot(kg\cdot K)^{-1}$
Walls	0.05	Polystyrene panel	0.037	20	1.45
	Thermal transmittance: 0.625 W/(m^2·K)				
Roof with PCM	0.003	Steel sheet	52	7860	500
	0.03	PCM panel	1.09 (solid state) 0.54 (liquid state)	1640	1440 (0–26.5°C) 125 000 (26.5°C–28°C) 1440 (28°C–60°C)
	0.003	Steel sheet	52	7860	500
	Thermal transmittance: 5.111 W/(m^2·K)				
Roof with air	0.003	Steel sheet	52	7860	500
	0.03	Air	0.024	1.23	1000
	0.003	Steel sheet	52	7860	500
	Thermal transmittance: 2.777 W/(m^2·K)				
Floor	0.015	Plywood	0.140	500	1.70
	Thermal transmittance: 2.985 W/(m^2·K)				

Table 5 Temperature-enthalpy data of BioPCM M27/Q21 [34]

Temperature/ °C	Enthalpy/ $J\cdot kg^{-1}$	Temperature/ °C	Enthalpy/ $J\cdot kg^{-1}$
–20	1	27	134 578
0	5	27.5	202 864
10	16 458	28	237 015
15	23 562	30	251 278
20	32 561	32	255 234
25	43 078	35	258 320
26	57 014	45	267 324
26.5	84 146	100	322 093

3. Results

3.1 Experimental validation

To evaluate the effect of the studied PCM in reducing the building heating load, we use the model introduced in the previous section 4 to simulate the indoor temperature of the two test rooms during the summer, fall, and winter periods. Results are presented in graphical figures for two consecutive days (48 hours) of each period, i.e. March 15th and 16th (summer), May 4th and 5th (fall), and July 09th and 10th (winter).

The temperature variations of the simulated and experimental interior air temperatures of both test rooms are shown in Fig. 9 and Fig. 10 respectively to compare the proposed model results with the experiment.

The interior air temperature of the air-panel test room shows a large fluctuation throughout the day as it is immediately influenced by the incident solar radiation. A small fluctuation of the room ceiling temperature is observed during night-time, showing the influence of the ambient air temperature in the ceiling temperature, although in a smaller proportion than the solar radiation. The interior air temperature of the air-panel room shows a good agreement with the measured temperatures. However, due to the assumptions made previously, the proposed model shows small errors during the afternoon in predicting temperatures. Indeed, values of interfacial resistance, and outside and inside convection coefficients, may be varying during the day, and the theoretical values may be different from the real values.

The interior air temperature of the PCM room shows a much smaller fluctuation (Fig. 10) than that of the air-panel test room (Fig. 9). From the experimental results, the increase in the interior air temperature of the PCM-panel room in the morning is also directly influenced by the incident solar radiation, but it is smaller than the one of the air-panel room, due to the higher specific heat of the PCM and the large heat storage capacity of the PCM. The interior air temperature of the PCM-panel room still increases in the afternoon when the solar radiation decreases, but at a smaller rate than in the morning. At night-time, the interior air temperature of the PCM test room decreases slowly during the solidification process rejecting the heat stored during the day to its surroundings.

The simulated interior air temperature of the PCM-panel room shows an acceptable agreement with the measured temperatures. Some small errors remain during the afternoon and night, as (1) the peak of simulated room temperature appears earlier than that of experimental data, and (2) the modeled indoor air temperature does not drop as much as the experimental room temperature when the sun disappears. This may be explained by various reasons. First, the room temperature is influenced by outside and inside room conditions. Wind conditions affect the outside convective heat

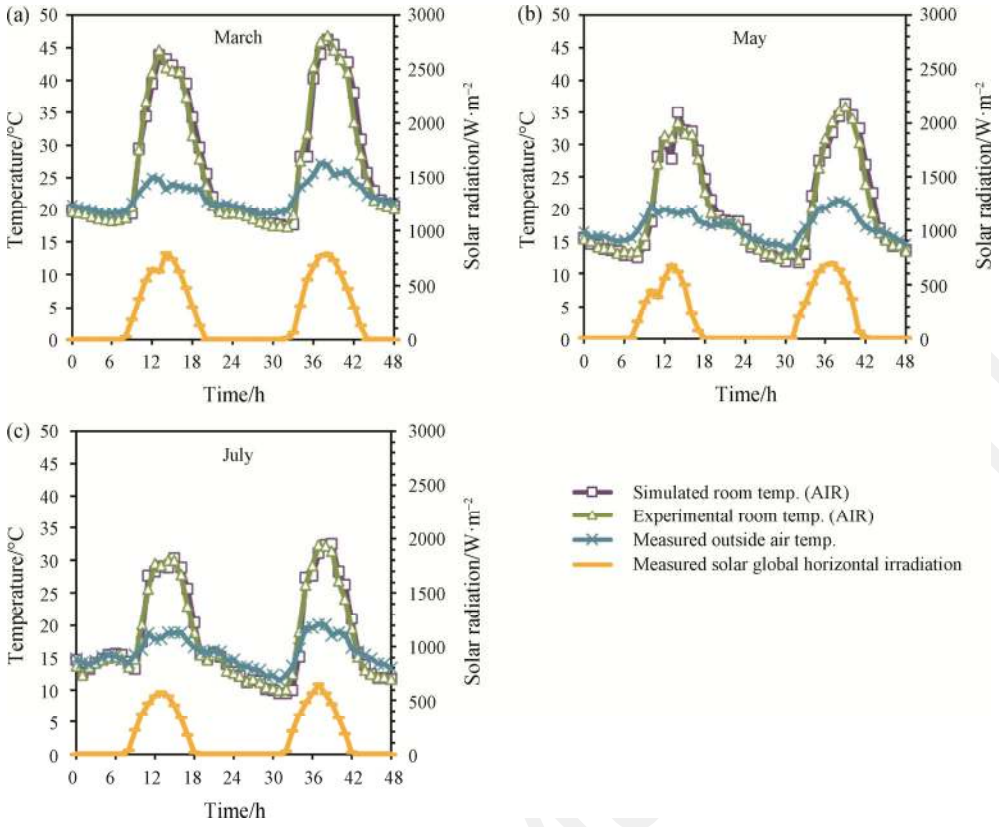

Fig. 9 Simulated and experimental interior temperatures of the air panel room in (a) summer, (b) fall, and (c) winter

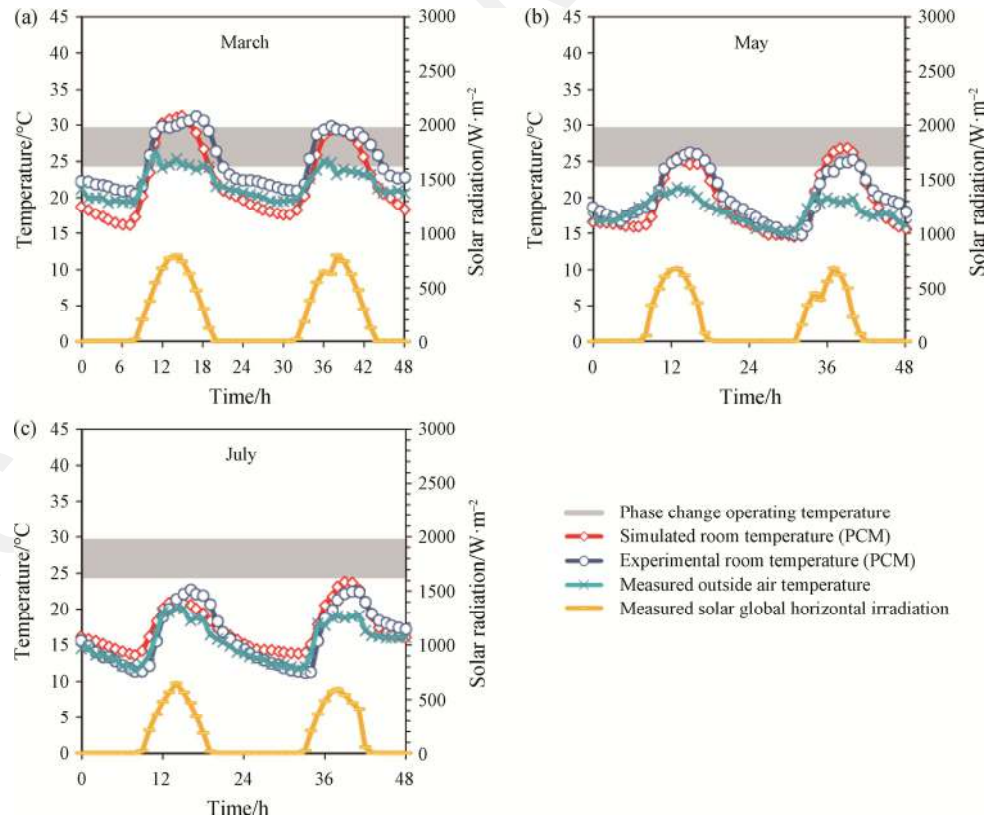

Fig. 10 Simulated and experimental temperatures of the PCM room in (a) summer, (b) fall, and (c) winter

transfer coefficient on one side, while on the other side, the room air permeability influences the heat transfer due to air ventilation, thus the indoor room temperature. Second, the heat conduction in the roof panel is not one-dimensional, and the end effect is influencing the heat conduction. In addition, other parameters which can explain the difference between simulated and experimental values, are: (1) the variation of the PCM thermal conductivity according to its temperature and phase; (2) the PCM is not homogenous and isotropic, which can affect the PCM effective thermal conductivity in the experiment; (3) the phase change does not occur at the prescribed temperature.

3.2 PCM performance in other climates

The indoor temperature of the PCM-panel test room was simulated for the same two consecutive days of each period as in the previous section 3.1. The results for the seven other cities are presented in Table 1.

Fig. 11 shows the simulated interior air temperatures of the PCM-panel room for the following climates: Desert (Calama), Semi Desert (Copiapó), and Maritime (Valparaiso). In general, it can be observed that in all cities the indoor temperature is always higher than the outdoor temperature. Also, the biggest differences between temperatures are in the summer and winter seasons.

Fig. 12 shows the simulated interior air temperatures of the PCM-panel room for the following climates: Mediterranean (Santiago), Maritime rainy (Concepción), Rainy and cold with frequent frosts (Temuco), and Rainy and cold (Punta Arenas). It can be observed that the biggest difference between indoor and outdoor temperatures occurs in summer and winter. While in fall, both temperatures show a similar behavior presenting only small differences.

In the case of Punta Arenas, the difference between the indoor and outdoor temperature is more than 5°C, and practically it is maintained throughout the day and night. This may be due to its location in the extreme south, where the outdoor ambient air temperature does not fluctuate throughout the day as much as in more central locations. While in other cities the greatest difference in temperature occurs during the hours close to midday.

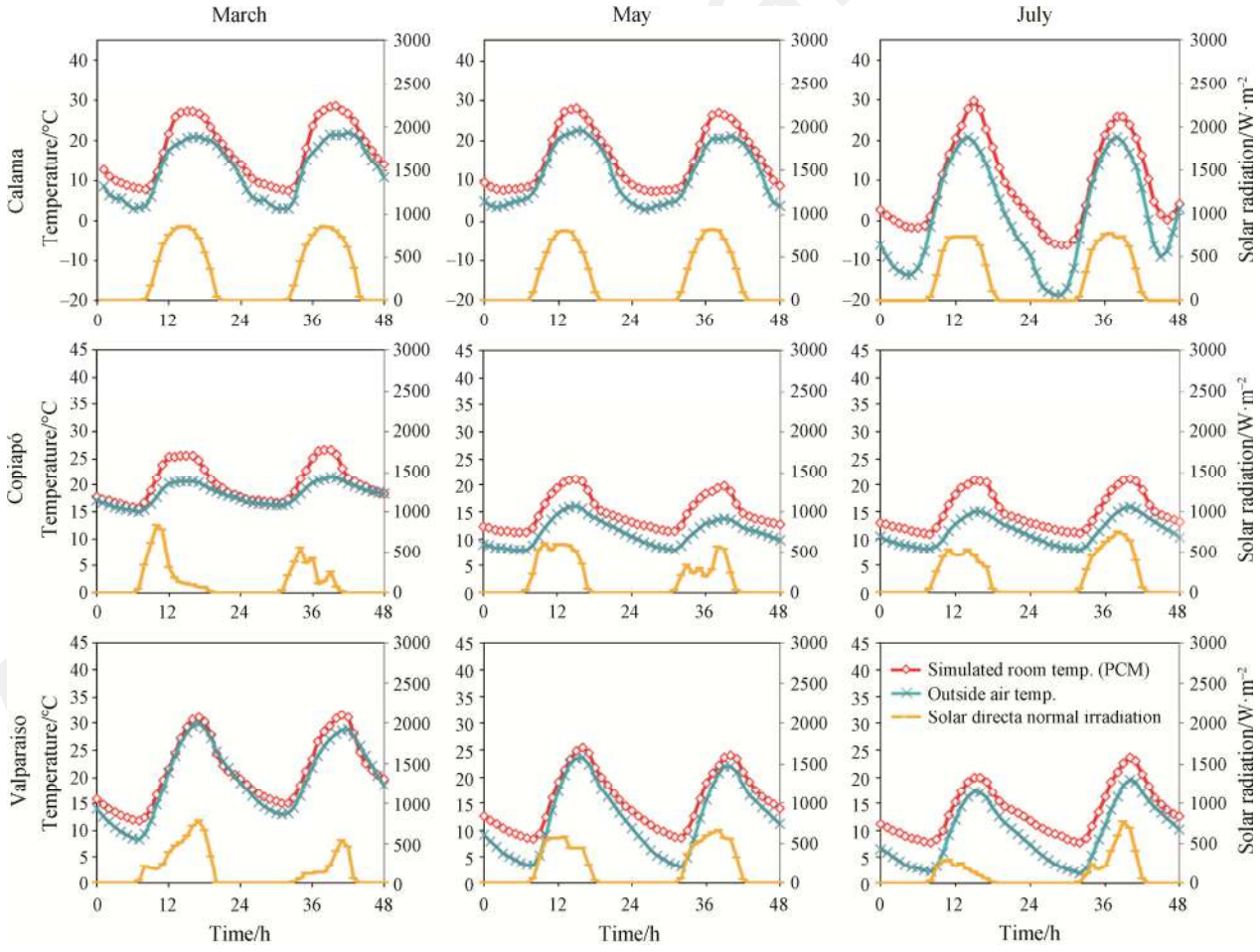

Fig. 11 Simulated temperatures of the PCM-panel room in Calama, Copiapó, and Valparaiso

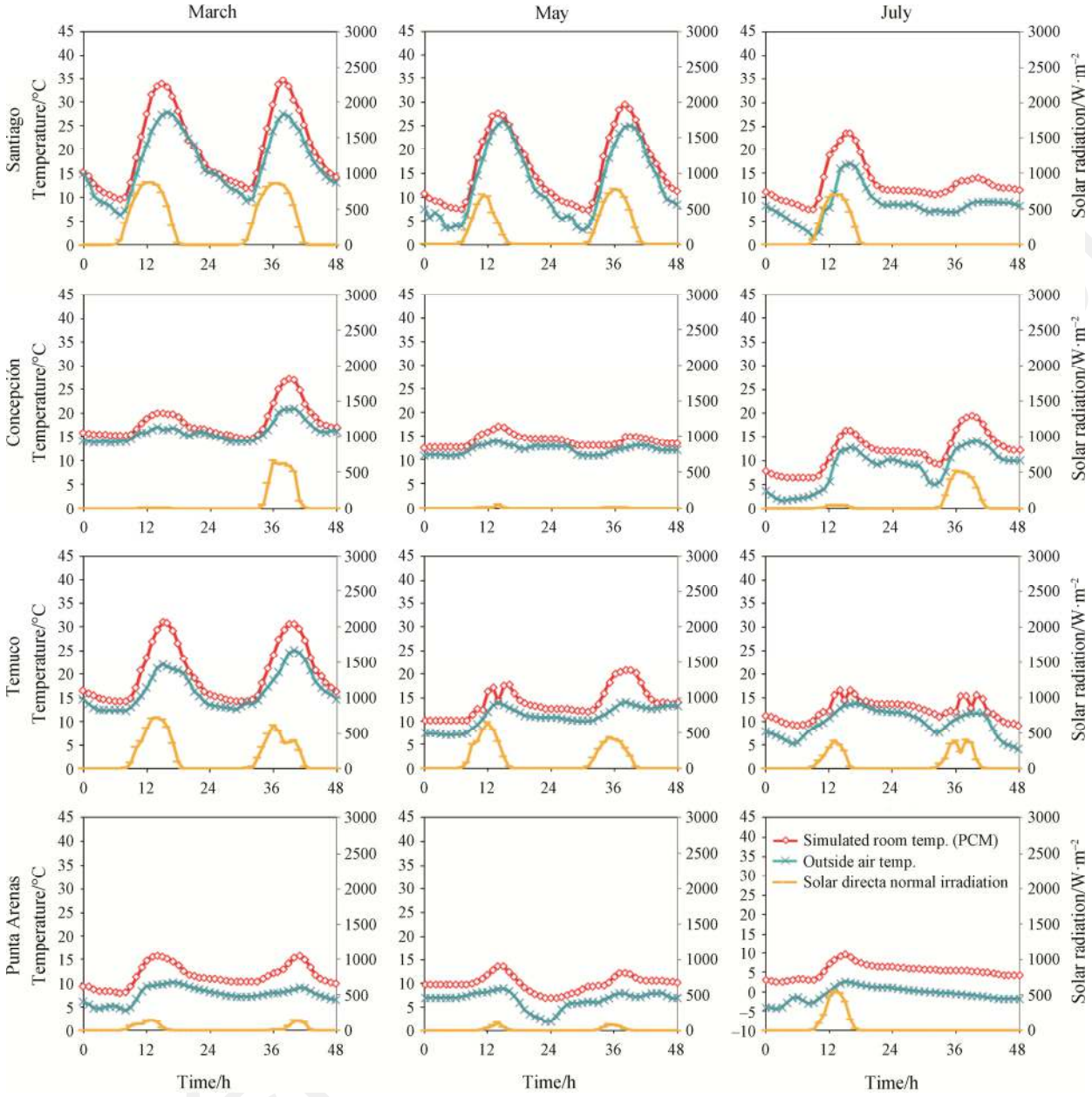

Fig. 12 Simulated temperatures of the PCM-panel room in Santiago, Concepción, Temuco, and Punta Arenas

In the case of Valparaiso and Concepción, the indoor and outdoor temperatures present small differences, except for some hours of the day in some of the seasons. This may be because both cities are located on the coast, where the ambient air temperature remains relatively more constant throughout the day than in inland cities (Calama, Copiapó, Santiago, and Temuco).

4. Discussion

One important finding of this research is that the PCM, used as a passive latent heat thermal energy storage system, can smooth diurnal indoor temperature fluctuations under the conditions of the experimental test rooms in Antofagasta (Fig. 9 and Fig. 10). Results show that the PCM is more effective in the winter period (i.e. July), as it can maintain the indoor air temperature within the range of thermal comfort, while in the summer period (i.e. March), the indoor air temperature rises to 28°C and above in most of the studied climates. Such observation is in good agreement with the results reported by Ramakrishnan et al. [44] on commercial PCMs. The increase in indoor air temperature is mainly explained by the incident solar radiation, but also by the absence of a mechanical ventilation system in the experimental test rooms. Indeed, the use of mechanical ventilation would

allow the indoor temperature to remain for longer durations within the comfort range in hot climates [45]. At least, the peak indoor air temperature could be reduced by the use of night ventilation, as shown by Al-Absi et al. [46].

The study shows that placing the PCM on the outer face of the building envelope, integrated into exterior insulation systems, can be an effective solution to store latent heat thermal energy for a wide range of climate locations. Indeed, the PCM was able to complete the full melting-freezing cycle daily in different seasons for various Chilean locations benefiting from (1) relatively acceptable levels of solar radiation during the day and (2) tempered/cold temperatures during the night. Placed in a single layer in direct contact with a 3 mm metal sheet, it could absorb the solar radiation heat during the day and melt. Then, it could slowly cool down and freeze again during the night because of the colder outside temperature. Further investigation should include the performance simulation of PCM-enhanced exterior insulation systems, in particular those conditioned in modular panels for implementation in new construction or in building retrofits.

The melting temperature and thickness of the PCM should be chosen based on climatic conditions of temperature and solar radiation so that all the PCM mass can be melted and frozen completely during a daily cycle. However, other factors such as the building envelope insulation, PCM surface orientation, building thermal inertia, internal loads, and the ventilation strategy must be taken carefully into consideration for choosing the most optimum melting temperature and thickness of the PCM [47]. For instance, a low melting temperature may result in a PCM under-utilization in the warmest months, when the PCM would not solidify. Analogously, a high melting temperature may reduce the effectiveness of the PCM in colder months, as the PCM would not melt.

Although the use of PCM in buildings reduces CO_2 emissions from heating and cooling energy use [48, 49], a balance has to be found to obtain the maximum annual energy savings over both the heating and cooling seasons. Ascione et al. [50] found that the greatest cooling energy savings were obtained in Mediterranean climates by installing the PCM plaster on all exposures of the building's vertical envelope and that the energy demand decreased with the increase of the PCM thickness. Also, Sovetova et al. [51] pointed out that, in hot desert climates, the higher energy savings occur during the summer months and found that the energy savings increased with the increase in the PCM surface area and decreased with the increase in the PCM layer thickness. In the case of an office building located in different cities in China, Mi et al. [52] highlighted that the best savings in energy consumption provided by the use of PCM occurred in the cold region as well as in hot summers and cold winters.

As the PCM performance is related to the activation of its phase change process, and thus its melting temperature, the same PCM does not offer the same benefits in both the heating and cooling energy demands. In this sense, hybrid systems consisting of two PCM of different melting temperatures have the potential to increase energy savings in both the heating and cooling seasons [53].

This research is a limited exploration of this topic. There is a strong need for further analysis, assessing the effects of different PCM configurations, orientations, and thicknesses on improving indoor comfort conditions, reducing heating and cooling energy use, and mitigating the effects of climate change.

5. Conclusions

The thermal performance of an inorganic eutectic PCM (48% $CaCl_2$+4.3% NaCl+0.4% KCl+47.3% H_2O) integrated into a rooftop slab of a test room located in Antofagasta (Chile) is analyzed by experimental and numerical investigation. The experiment is also conducted in a second test room, in which the rooftop panel is a sealed air cavity. The proposed modeling tool is developed using the finite difference method and validated using experimental data. It allows us to evaluate the effect of both the PCM and air rooftop panels on the room's thermal behavior.

The data collected in Antofagasta during the summer, fall, and winter periods show that the indoor temperature of the PCM room varies only 21.1°C±10.6°C, while the one of the air-panel room varies 28.3°C±18.5°C. Under the experiment's conditions, the PCM room's indoor temperature observes smoother diurnal fluctuations, with lower maximum and higher minimum indoor temperatures than that of the air-panel room. This is explained by the higher thermal mass and the thermal storage capacity of the PCM. Indeed, heat gains by solar radiation can be stored as latent heat in the PCM, while the solar radiation contributes to an increase of the air-panel room temperature as the effect of sensible heat gains. Thus, building elements incorporating PCM can be suitable for the improvement of the indoor thermal comfort and energy efficiency of buildings. In Antofagasta, it can smooth diurnal indoor temperature fluctuations, thus reducing the energy demand for space heating and cooling.

In the case of simulations in other climates, the study shows that the PCM panel has a better thermal performance during the winter period, as it helps to maintain or increase the room temperature by some degrees to reach comfort temperatures.

The paper contributes to filling the gap in experimental and numerical investigation related to the use of the studied PCM for latent heat thermal energy storage and energy conservation in Chilean buildings. It provides the building sector's stakeholders with scientifically-based evidence that the implementation of such PCM in the building envelope can effectively reduce space heating and cooling needs, and improve indoor thermal comfort in different climates of Chile.

Acknowledgment

The authors gratefully acknowledge the research support provided by CEDEUS (ANID/FONDAP 1522A0002), SERC (ANID/FONDAP 1522A0006), and the UAI Earth Research Centre. Also, the authors extend their gratitude to FAVE Project, Code: 2018-2019-3C1-069, funded by FONDOCyT 2018-2019, Ministry of Higher Education Science, and Technology (MESCyT). F.S. acknowledges support from ANID/FONDECYT 3210690.

Funding

This work was supported by ANID/FONDAP 1522A0002, ANID/FONDECYT 3210690, MESCyT/FONDOCyT 2018-2019-3C1-069, ANID/FONDAP 1522A0006, and the UAI Earth Research Center.

Conflict of Interest

On behalf of all authors, the corresponding author states that there is no conflict of interest.

References

[1] Ministry of Energy, Informe Balance Nacional de Energía 2020, Santiago, Chile, 2022. https://energia.gob.cl/sites/default/files/documentos/2022_informe_anual_bne_2020.pdf.

[2] InData SpA, CDT, Usos de energía de los hogares de Chile 2018. Informe Final, Santiago, Chile, 2019. https://www.energia.gob.cl/sites/default/files/documentos/informe_final_caracterizacion_residencial_2018.pdf.

[3] Simon F., Ordoñez J., Girard A., Parrado C., Modelling energy use in residential buildings: How design decisions influence final energy performance in various Chilean climates. Indoor and Built Environment, 2019, 28: 533–551. https://doi.org/10.1177/1420326X18792661.

[4] Chan A., Energy and environmental performance of building facades integrated with phase change material in subtropical Hong Kong. Energy and Buildings, 2011, 43: 2947–2955. https://doi.org/10.1016/j.enbuild.2011.07.021.

[5] Nghana B., Tariku F., Phase change material's (PCM) impacts on the energy performance and thermal comfort of buildings in a mild climate. Building and Environment, 2016, 99: 221–238. https://doi.org/10.1016/j.buildenv.2016.01.023.

[6] Cabeza L.F., Castellón C., Nogués M., Medrano M., Leppers R., Zubillaga O., Use of microencapsulated PCM in concrete walls for energy savings. Energy and Buildings, 2007, 39: 113–119. https://doi.org/10.1016/j.enbuild.2006.03.030.

[7] Baetens R., Jelle B.P., Gustavsen A., Phase change materials for building applications: A state-of-the-art review. Energy and Buildings, 2010, 42: 1361–1368. https://doi.org/10.1016/j.enbuild.2010.03.026.

[8] Barreneche C., Navarro M.E., Fernández A.I., Cabeza L.F., Improvement of the thermal inertia of building materials incorporating PCM. Evaluation in the macroscale. Applied Energy, 2013, 109: 428–432. https://doi.org/10.1016/j.apenergy.2012.12.055.

[9] Mandilaras I.D., Kontogeorgos D.A., Founti M.A., A hybrid methodology for the determination of the effective heat capacity of PCM enhanced building components. Renewable Energy, 2015, 76: 790–804. https://doi.org/10.1016/j.renene.2014.11.078.

[10] Kośny J., PCM-Enhanced building components: An application of phase change materials in building envelopes and internal structures. Cham: Springer International Publishing, 2015. https://doi.org/10.1007/978-3-319-14286-9.

[11] Chandel S.S., Agarwal T., Review of current state of research on energy storage, toxicity, health hazards and commercialization of phase changing materials. Renewable and Sustainable Energy Reviews, 2017, 67: 581–596. https://doi.org/10.1016/j.rser.2016.09.070.

[12] Athienitis K., Liu C., Hawes D., Banu D., Feldman D., Investigation of the thermal performance of a passive solar test-room with wall latent heat storage. Building and Environment, 1997, 32(5): 405–410. https://doi.org/10.1016/S0360-1323(97)00009-7.

[13] Evola G., Marletta L., Sicurella F., A methodology for investigating the effectiveness of PCM wallboards for summer thermal comfort in buildings. Building and Environment, 2013, 59: 517–527. https://doi.org/10.1016/j.buildenv.2012.09.021.

[14] Castell A., Martorell I., Medrano M., Pérez G., Cabeza L.F., Experimental study of using PCM in brick constructive solutions for passive cooling. Energy and Buildings, 2010, 42: 534–540. https://doi.org/10.1016/j.enbuild.2009.10.022.

[15] Kośny J., Fallahi A., Shukla N., Kossecka E., Ahbari R., Thermal load mitigation and passive cooling in

residential attics containing PCM-enhanced insulations. Solar Energy, 2014, 108: 164–177. https://doi.org/10.1016/j.solener.2014.05.007.

[16] Xu T., Chen Q., Zhang Z., Gao X., Huang G., Investigation on the properties of a new type of concrete blocks incorporated with PEG/SiO_2 composite phase change material. Building and Environment, 2016, 104: 172–177. https://doi.org/10.1016/j.buildenv.2016.05.003.

[17] Akeiber H., Nejat P., Majid M.Z.A., Wahid M.A., Jomehzadeh F., Famileh I.Z., Calautit J.K., Hughes B.R., Zaki S.A., A review on phase change material (PCM) for sustainable passive cooling in building envelopes. Renewable and Sustainable Energy Reviews, 2016, 60: 1470–1497. https://doi.org/10.1016/j.rser.2016.03.036.

[18] Zhang Y., Zhou G., Lin K., Zhang Q., Di H., Application of latent heat thermal energy storage in buildings: State-of-the-art and outlook. Building and Environment, 2007, 42: 2197–2209. https://doi.org/10.1016/j.buildenv.2006.07.023.

[19] Fatih Demirbas M., Thermal energy storage and phase change materials: An overview. Energy Sources, Part B: Economics, Planning, and Policy, 2006, 1: 85–95. https://doi.org/10.1080/009083190881481.

[20] Jin X., Zhang S., Xu X., Zhang X., Effects of PCM state on its phase change performance and the thermal performance of building walls. Building and Environment, 2014, 81: 334–339. https://doi.org/10.1016/j.buildenv.2014.07.012.

[21] Rodríguez-Ubinas E., Ruiz-Valero L., Vega S., Neila J., Applications of phase change material in highly energy-efficient houses. Building and Environment, 2012, 50: 49–62. https://doi.org/10.1016/j.enbuild.2012.03.018.

[22] Rodríguez-Ubiñas E., Ruíz-Valero L., Sánchez S.V., Neila González F.J., Latent heat thermal energy storage systems in lightweight construction: Review of PCM applications in solar decathlon houses. WIT Transactions on Ecology and the Environment, 2011, 150: 935–946. https://doi.org/10.2495/SDP110781.

[23] Yu X., Chang J., Huang R., Huang Y., Lu Y., Li Z., Wang L., Sensitivity analysis of thermophysical properties on PCM selection under steady and fluctuating heat sources: A comparative study. Applied Thermal Engineering, 2021, 186: 116527. https://doi.org/10.1016/j.applthermaleng.2020.116527.

[24] Cui Y., Xie J., Liu J., Pan S., Review of phase change materials integrated in building walls for energy saving. Procedia Engineering, 2015, 121: 763–770. https://doi.org/10.1016/j.proeng.2015.09.027.

[25] Delgado J.M., Martinho J.C., Sá A.V., Guimarães A.S., Abrantes V., Thermal energy storage with phase change materials: A literature review of applications for buildings materials. Springer Cham, 2018. https://doi.org/10.1007/978-3-319-97499-6.

[26] Trunilina A.V., Baurova N.I., Polymer composites with biodegradative properties. Polymer Science, Series D, 2019, 12: 167–169. https://doi.org/10.1134/S1995421219020230.

[27] Palacios A., De Gracia A., Haurie L., Cabeza L.F., Fernández A.I., Barreneche C., Study of the thermal properties and the fire performance of flame retardant-organic PCM in bulk form. Materials, 2018, 11(1): 117. https://doi.org/10.3390/ma11010117.

[28] Nazir H., Batool M., Bolivar Osorio F.J., Isaza-Ruiz M., Xu X., Vignarooban K., Phelan P., Inamuddin, Kannan A.M., Recent developments in phase change materials for energy storage applications: A review. International Journal of Heat and Mass Transfer, 2019, 129: 491–523. https://doi.org/10.1016/j.ijheatmasstransfer.2018.09.126.

[29] Mahdi J.M., Lohrasbi S., Nsofor E.C., Hybrid heat transfer enhancement for latent-heat thermal energy storage systems: A review. International Journal of Heat and Mass Transfer, 2019, 137: 630–649. https://doi.org/10.1016/j.ijheatmasstransfer.2019.03.111.

[30] BCN, Información Territorial, Bibl. Del Congr. Nac. Chile. (2022). https://www.bcn.cl/siit/nuestropais/region2/region2 (accessed June 1, 2022).

[31] MMA, Base digital del clima, Minist. Del Medio Ambient. Gob. Chile. (2022). http://basedigitaldelclima.mma.gob.cl/study/one/zones/34 (accessed June 1, 2022).

[32] Weather Spark, El clima promedio en Antofagasta, Cedar Lake Ventur. Inc. (2022). https://es.weatherspark.com/y/26546/Clima-promedio-en-Antofagasta-Chile-durante-todo-el-año (accessed June 1, 2022).

[33] Molina A., Falvey M., Rondanelli R., A solar radiation database for Chile. Scientific Reports, 2017, 7: 1–11. https://doi.org/10.1038/s41598-017-13761-x.

[34] DesignBuilder, DesignBuilder v5.0.2.3, (2018). https://designbuilder.co.uk/.

[35] SCS Arquitecto Spa, Guía Buiclimática. Zonas climáticas del Chile Continental, (2018). https://scsarquitecto.cl/guia-bioclimatica-zonas-climaticas-chile-continental/ (accessed July 6, 2022).

[36] Sharma A., Tyagi V.V., Chen C.R., Buddhi D., Review on thermal energy storage with phase change materials and applications. Renewable and Sustainable Energy Reviews, 2009, 13(2): 318–345. https://doi.org/10.1016/j.rser.2007.10.005.

[37] Kuznik F., Virgone J., Experimental assessment of a phase change material for wall building use. Applied Energy, 2009, 86: 2038–2046.

https://doi.org/10.1016/j.apenergy.2009.01.004.

[38] Boemi S.N., Irulegi O., Santamouris M., Energy performance of buildings: Energy efficiency and built environment in temperate climates. Cham: Springer International Publishing, 2016. https://doi.org/10.1007/978-3-319-20831-2.

[39] US Department of Energy, EnergyPlus energy simulation software (version 8.7.0), 2018. https://energyplus.net/.

[40] Tabares-Velasco P.C., Christensen C., Bianchi M., Verification and validation of EnergyPlus phase change material model for opaque wall assemblies. Building and Environment, 2012, 54: 186–196. https://doi.org/10.1016/j.buildenv.2012.02.019.

[41] Auzeby M., Wei S., Underwood C., Tindall J., Chen C., Ling H., Buswell R., Effectiveness of using phase change materials on reducing summer overheating issues in UK residential buildings with identification of influential factors. Energies, 2016, 9(8): 605. https://doi.org/10.3390/en9080605.

[42] Ozdenefe M., Dewsbury J., Dynamic thermal simulation of a PCM lined building with energy plus. Proceedings of 7th WSEAS International Conference on Energy and Environment, Kos Island, Greece, 2012, pp. 359–364.

[43] Neila González F.J., Arquitectura bioclimática en un entorno sostenible. Editorial Munilla-Lería, Madrid, 2004.

[44] Ramakrishnan S., Wang X., Sanjayan J., Wilson J., Thermal performance assessment of phase change material integrated cementitious composites in buildings: Experimental and numerical approach. Applied Energy, 2017, 207: 654–664. https://doi.org/10.1016/j.apenergy.2017.05.144.

[45] Salihi M., El Fiti M., Harmen Y., Chhiti Y., Chebak A., M'Hamdi Alaoui F.E., Achak M., Bentiss F., Jama C., Evaluation of global energy performance of building walls integrating PCM: Numerical study in semi-arid climate in Morocco. Case Studies in Construction Materials, 2022, 16: e00979. https://doi.org/10.1016/j.cscm.2022.e00979.

[46] Al-Absi Z.A., Mohd Hafizal M.I., Ismail M., Mardiana A., Ghazali A., Peak indoor air temperature reduction for buildings in hot-humid climate using phase change materials. Case Studies in Thermal Engineering, 2020, 22: 100762. https://doi.org/10.1016/j.csite.2020.100762.

[47] Bhamare D.K., Rathod M.K., Banerjee J., Numerical model for evaluating thermal performance of residential building roof integrated with inclined phase change material (PCM) layer. Journal of Building Engineering, 2020, 28: 101018. https://doi.org/10.1016/j.jobe.2019.101018.

[48] Mohseni E., Tang W., Parametric analysis and optimisation of energy efficiency of a lightweight building integrated with different configurations and types of PCM. Renewable Energy, 2021, 168: 865–877. https://doi.org/10.1016/j.renene.2020.12.112.

[49] Kabdrakhmanova M., Memon S.A., Saurbayeva A., Implementation of the panel data regression analysis in PCM integrated buildings located in a humid subtropical climate. Energy, 2021, 237: 121651. https://doi.org/10.1016/j.energy.2021.121651.

[50] Ascione F., Bianco N., De Masi R.F., de' Rossi F., Vanoli G.P., Energy refurbishment of existing buildings through the use of phase change materials: Energy savings and indoor comfort in the cooling season. Applied Energy, 2014, 113: 990–1007. https://doi.org/10.1016/j.apenergy.2013.08.045.

[51] Sovetova M., Memon S.A., Kim J., Thermal performance and energy efficiency of building integrated with PCMs in hot desert climate region. Solar Energy, 2019, 189: 357–371. https://doi.org/10.1016/j.solener.2019.07.067.

[52] Mi X., Liu R., Cui H., Memon S.A., Xing F., Lo Y., Energy and economic analysis of building integrated with PCM in different cities of China. Applied Energy, 2016, 175: 324–336. https://doi.org/10.1016/j.apenergy.2016.05.032.

[53] Said M.A., Hassan H., Impact of energy storage of new hybrid system of phase change materials combined with air-conditioner on its heating and cooling performance. Journal of Energy Storage, 2021, 36: 102400. https://doi.org/10.1016/j.est.2021.102400.